NOTES AND CORRESPONDENCE

The Latitude-Height Structure of 40–50 Day Variations in Atmospheric Angular Momentum

JOHN R. ANDERSON[1]

Department of Meteorology and Physical Oceanography, M.I.T., Cambridge, MA 02139

RICHARD D. ROSEN

Atmospheric and Environmental Research, Inc., Cambridge, MA 02139

30 August 1982 and 7 February 1983

ABSTRACT

Quasi-periodic variations in the relative angular momentum of the atmosphere on time scales of around 40–50 days have been observed by Langley *et al.* (1981). A description of the two-dimensional (latitude–height) structure of the winds responsible for these changes is constructed here from five years of NMC twice-daily global analyses. Using cross-spectral and amplitude-phase eigenvector techniques, we find these variations are associated with wavelike motions in the tropical upper troposphere that propagate poleward and downward in phase within the tropics. A coherently connected midlatitude Northern Hemisphere component is also present whose phase is essentially independent of height. We believe the tropical component to be the zonally averaged part of the motions described by Madden and Julian (1971, 1972). The Northern Hemisphere midlatitude component may be a direct response to the tropical motions or both motions may be the common response to an as yet unidentified tropical forcing.

1. Introduction

Estimates of the relative angular momentum M of the atmosphere (below 100 mb) have been presented on a twice-daily basis for 1976–80 by Rosen and Salstein (1983). The time series of M exhibits quasi-periodic variations with periods of 40–50 days. Comparable variations have also been detected in measurements of the rotation rate of the earth, consistent with the assumption that the total angular momentum of the earth-atmosphere system is conserved on this time scale (Langley *et al.*, 1981). The work presented here is an attempt to determine the spatial structure of the atmospheric motions associated with these 40–50 day variations. In particular, we wish to determine the relationship between these variations in M and those in tropical motions with similar time scales reported by Madden and Julian (1971, 1972). More recent observational evidence for these wind variations have been offered by Anderson (1982) and Weickmann (1982). Because a zonally averaged data set was available to us which significantly reduced our computational requirements, we decided to examine only the two-dimensional structure of the winds. We realize, however, that many questions about the dynamics of the 40–50 day variations cannot be answered until a more complete study is performed that examines the longitudinal structure of the wind field.

2. Analysis techniques and results

Our data set has been derived from the National Meteorological Center (NMC) twice-daily global analyses and consists of zonally averaged values of the zonal wind at 10 pressure levels from 1000 to 100 mb at every 2.5° of latitude. These data have been used (Rosen and Salstein, 1983) to compute the angular momentum of the atmosphere about the polar axis relative to an earth-fixed frame, assuming the atmosphere to be in hydrostatic equilibrium with a surface pressure of 1000 mb:

$$M = \frac{2\pi a^3}{g} \int_{1000\text{ mb}}^{100\text{ mb}} \int_{\pi/2}^{-\pi/2} [u] \cos^2\phi \, d\phi dp,$$

where a is the radius of the earth, g is acceleration due to gravity, $[u]$ is the zonally averaged eastward component of the wind, ϕ is latitude, and p is pressure.

In Fig. 1, we present the time series of M for 1976–80 along with values of an independent measurement of changes in the earth's rotation rate [see Rosen and Salstein (1983) for further details]. The agreement between the two curves on time scales of less than a year or so is quite good and provides us with some measure of confidence in the zonal wind data. However, the sudden transition during September 1976 from anomalously low values of M is somewhat suspect, being traceable in part to questionable behavior in the NMC wind analysis over Southern Hemisphere high latitudes at this time (Anderson, 1982). Because the presence of this transition would adversely impact

[1] Present affiliation: Department of Atmospheric Sciences, Colorado State University, Fort Collins.

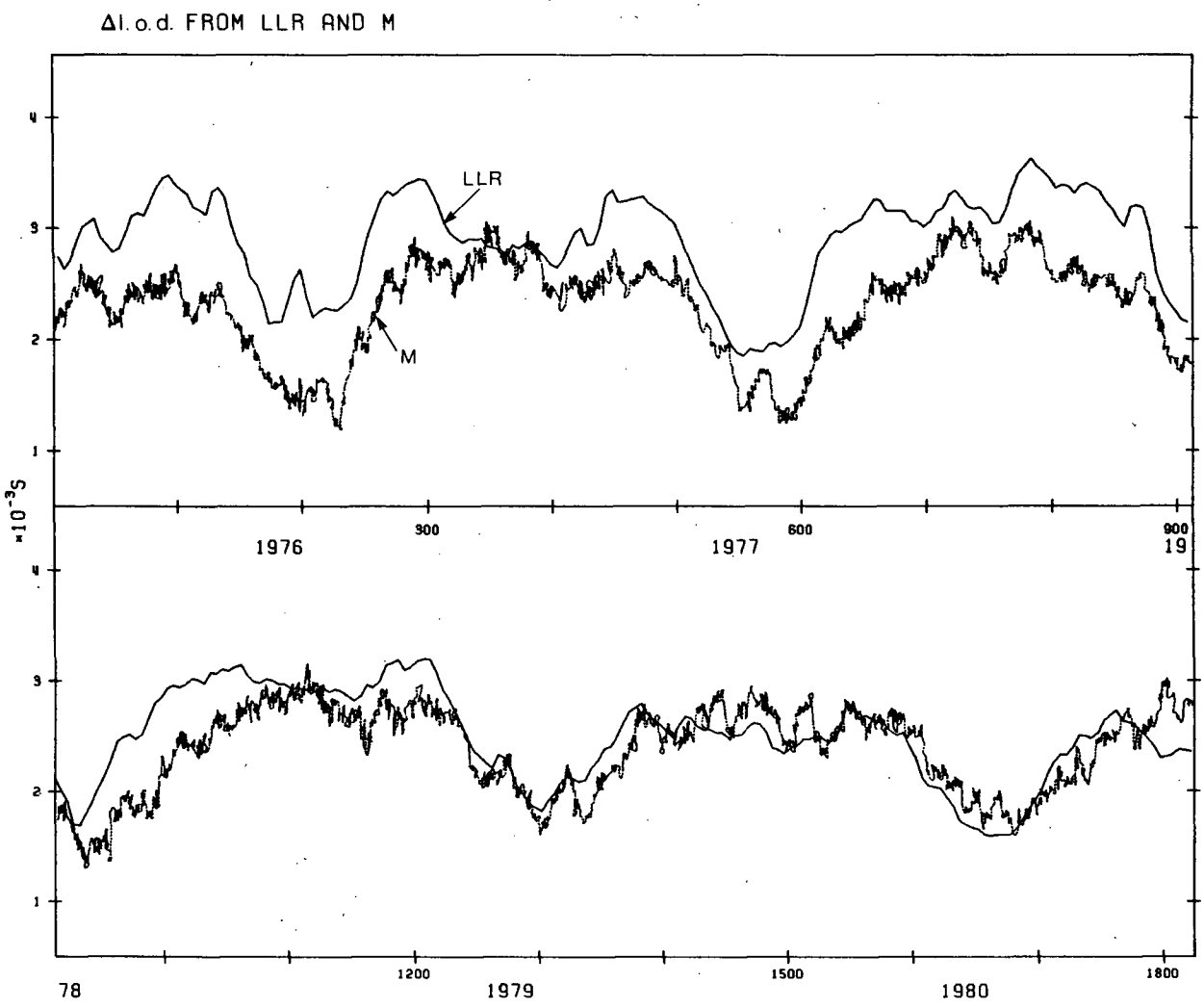

FIG. 1. Variations in the length of day (l.o.d.) during 1976–80 determined from lunar laser ranging observations (solid line) and inferred from M (dashed line) through the relationship Δl.o.d. (s) = $1.68 \times 10^{-29} \Delta M$ (kg m^2 s^{-1}). Time is marked in units of days from 1 January 1976. The fortnightly and monthly tidal terms in the lunar laser ranging values have been removed. The two curves have been displaced relative to each other by an arbitrary constant amount. (Taken from Rosen and Salstein, 1983.)

our study of 40–50 day fluctuations in M, we have chosen to use data only after this event in the remainder of our analysis.

Before attempting to determine the spectral components of the M time series, we first removed the large annual signal by subtracting the mean seasonal cycle for 1977–80 from each value of M. The resulting series of M anomaly values is shown in Fig. 2 for the period from October 1976 through December 1980. Estimates of the power spectrum of this series were computed in two ways. First, a classical Blackman–Tukey (1959) spectral estimate was made using the optimal window proposed by Papoulis (1973), which yields the result shown in Fig. 3. The second estimate uses an autoregressive (maximum entropy) model originally proposed by Burg (1975) with a least-squares prediction error filter (Marple, 1980). This estimate is given in Fig. 4. The two spectra closely resemble each other and are consistent with behavior having a red noise background with unresolved long-period components and a rather broad peak at periods of 40–50 days. There is also some evidence for significant peaks at 17 days and shorter; however, the spatial structure associated with these peaks is difficult to study because of their small amplitudes.

To isolate the 40–50 day motions, a band-pass filter was constructed with the frequency response given in Fig. 5 and then applied to our zonal wind anomaly data. The filter has an impulse response length of 179 days and does not distort the phase of the input wind data. A detailed description of the design and properties of such a zero-phase filter is given by Oppenheim and Schafer (1975). The time series of M values associated with the filtered winds is given in Fig. 6.

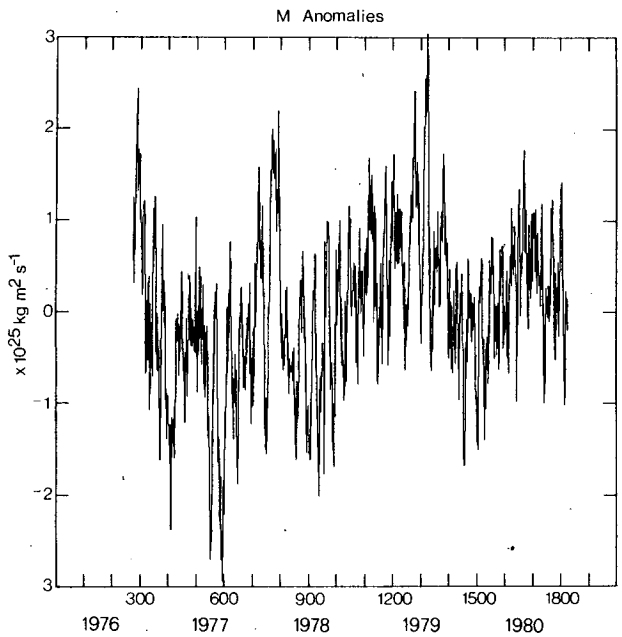

FIG. 2. Time series of daily global M anomalies used in this study.

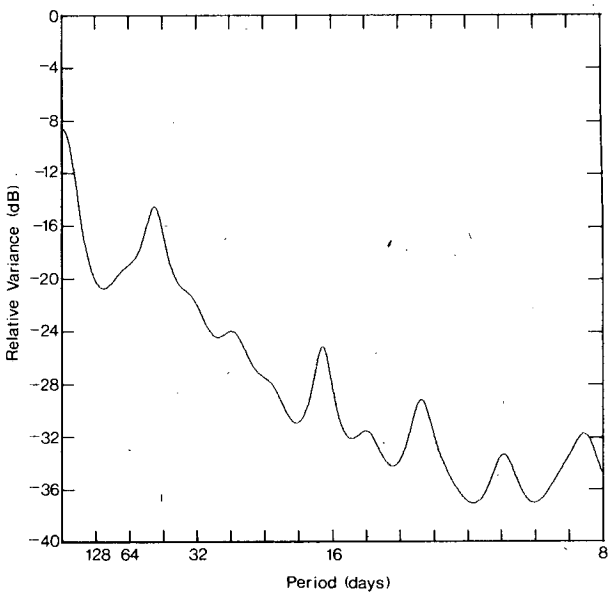

FIG. 4. Maximum Entropy Method (order 30) estimate of the M anomaly time series variance spectrum using a least-squares prediction error filter.

Note that the phase and amplitude of the oscillation appear to vary randomly with no obvious relationship to season.

The standard deviation of the band-pass winds is plotted as a function of latitude and height in Fig. 7. The 40–50 day fluctuation appears not to be exclusively tropical, and its largest amplitudes seem to occur in the upper troposphere. We are interested, of course, in determining what processes, if any, link the various regions of high variability. In particular, are propagating atmospheric waves of some sort involved?

To detect the presence of propagating phenomena, it is often useful to begin by constructing a time series from one's data that has the same power as the original series but is phase-shifted by 90°. Such a series is usually referred to as a Hilbert transform (HT) of

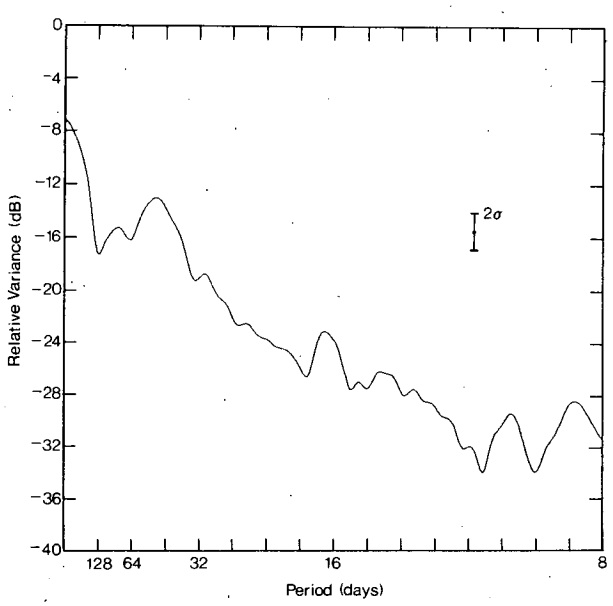

FIG. 3. Blackman–Tukey estimate of the M anomaly time series variance spectrum using a Papoulis autocorrelation window. Variance units are arbitrary and an estimate of the 95% level of significance is given by the vertical bar.

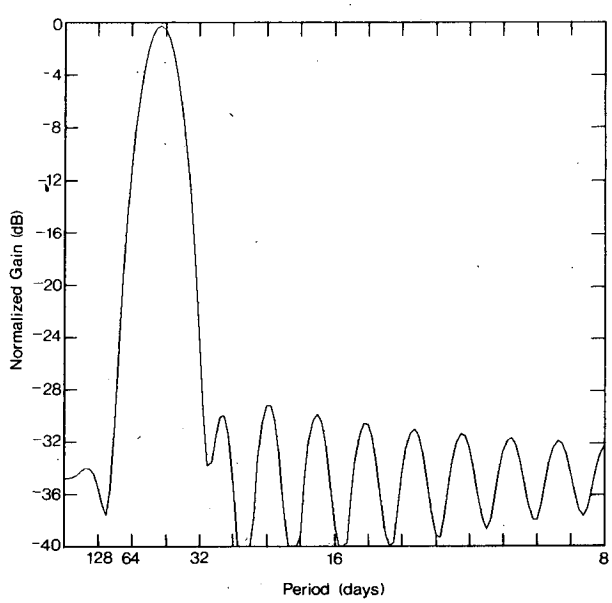

FIG. 5. Power (variance) response of the 45-day band-pass filter.

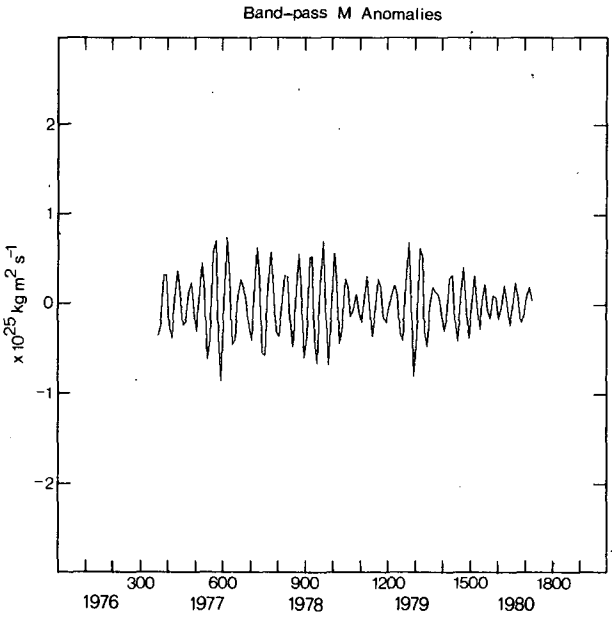

FIG. 6. Time series of 45-day band-pass filtered M anomalies, sampled at 15-day intervals.

the original series. [A detailed discussion of the construction of Hilbert transforms is also given by Oppenheim and Schafer (1975).] An HT of the band-pass M series was constructed with care taken to ensure that it would be orthogonal to the M series on the sampling interval used (30 days). Since the Nyquist sampling interval for the output from our band-pass filter is ~50 days, our choice of 30-day samples for the HT transform is sufficient and aliases the peak of the filter's frequency response near the center of the band-pass spectrum.

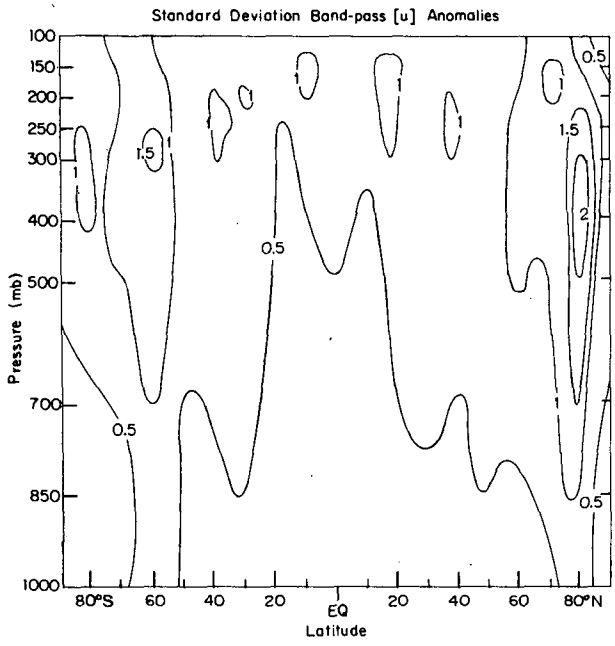

FIG. 7. Latitude-height cross section of the standard deviation of the 45-day band-pass filtered [u] anomalies. Units are m s^{-1}.

The properties of Hilbert transforms permit one to define a generalized correlation coefficient between two series that accounts not only for the strength of the relationship but also its phase. In our case, we write this complex correlation coefficient $\boldsymbol{r}$ as

$$\boldsymbol{r} = Ae^{i\pi\rho},$$

where $A = (x^2 + y^2)^{1/2}$, $\rho = \pi^{-1} \tan^{-1}(y/x)$ $(-1 \leqslant \rho \leqslant 1)$, x is the simple correlation coefficient between the band-pass winds and the M series constructed from them, and y is the simple correlation coefficient between the band-pass winds and the HT of the M series. The correlation amplitude A is the square root of the squared coherency of the cross spectrum at the band-pass frequency between the two series when computed with a frequency resolution equal to the filter bandwidth (Chatfield, 1980).

Fig. 8 shows the correlation amplitude A and phase ρ between the time series of band-pass winds and the M series in Fig. 6 at each point of the latitude–height grid. For the number of degrees of freedom associated with our band-pass filtered data set (~28), the correlation amplitude is significant at the 95% level of confidence for values of about 0.4 and greater (Goodman *et al.*, 1961). The sign convention in the correlation phase map is such that phase propagation is in the direction of increasing values. The apparent discontinuity in the correlation phase around 45°N results from defining ρ in terms of its principal value (*i.e.*, $-1 \leqslant \rho \leqslant 1$).

Fig. 8 depicts a strongly correlated tropical component in the upper troposphere with a well-defined minimum just north of the equator and maxima immediately to its north and south. The phase propagation is downward and toward both poles, with the southward propagation halting around 20°S. The propagation in the Northern Hemisphere branch also extends to ~20° beyond the equator. Unlike the Southern Hemisphere, however, the Northern Hemisphere tropical phenomenon is linked to a midlatitude component, which is centered near 40°N. The link appears to involve a nearly standing wave process, as evidenced by the $\sim\pi$ relative phase differences between the Northern Hemisphere subtropics and midlatitudes.

It should now be clear that the phenomenon we are studying is global in extent. To characterize its structure further, we employ a generalized version of the common eigenvector or empirical orthogonal function (EOF) analysis technique. This is accomplished by using an augmented data set consisting of the band-pass winds and their Hilbert transforms to

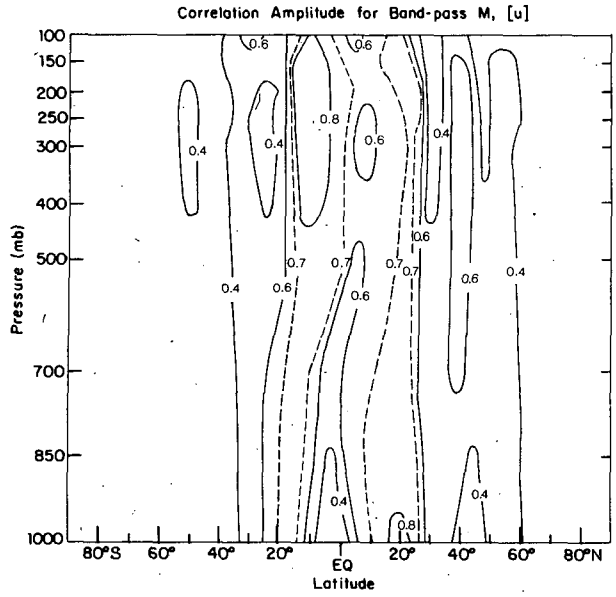

FIG. 8a. Cross section of the amplitude A of the complex correlation coefficient between the band-pass filtered M anomalies and the band-pass filtered $[u]$ anomalies at each grid point. Only amplitudes judged to be statistically significant, *i.e.*, greater than 0.4, are plotted.

help produce EOF's that depict the amplitude and phase of the variations in the data. In particular, these amplitude–phase EOF's allow coherently propagating waves to be represented compactly and efficiently. The amplitude–phase EOF technique proceeds by

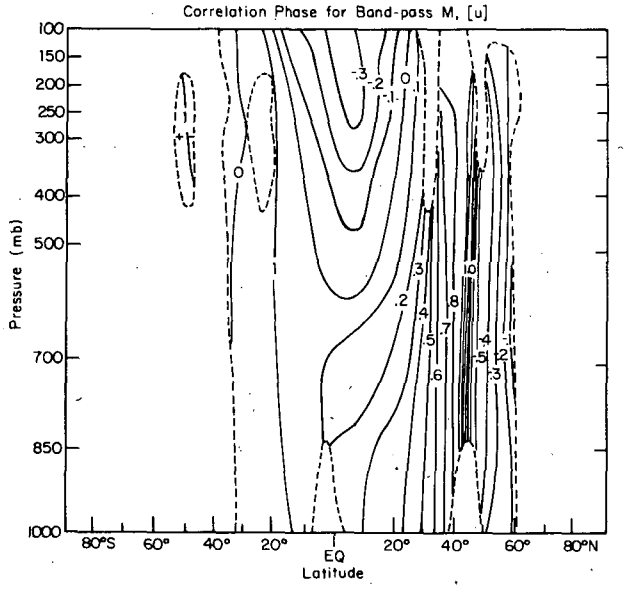

FIG. 8b. Cross section of the phase ρ of the complex correlation coefficient corresponding to Fig. 8a. Values are plotted only within the dashed lines where the correlation amplitude exceeds 0.4.

making the following approximation to the wind field:

$$[\hat{u}](\mathbf{x}, t) = \sum_{n=1}^{N} [A_n(\mathbf{x})I_n(t) + B_n(\mathbf{x})Q_n(t)],$$

where $\mathbf{x}$ is the spatial coordinate, t time, N the number of eigenvectors used in the expansion and Q is constrained to be the HT of I. The values of A, B and I are calculated by minimizing the mass-weighted squared error in the above approximation, in a manner similar to that followed in the traditional EOF approach. We can then define spatial amplitude and phase fields associated with each EOF, where the phase propagation convention is the same as that adopted above for the correlation analysis:

$$\text{amp}_n(\mathbf{x}) = [A_n^2(\mathbf{x}) + B_n^2(\mathbf{x})]^{1/2},$$

$$\text{phase}_n(\mathbf{x}) = \tan^{-1}\left(\frac{B_n(\mathbf{x})}{A_n(\mathbf{x})}\right).$$

The technique used here closely resembles the Hilbert singular decomposition method used by Rasmusson *et al.* (1981), and a more detailed description is given in a forthcoming work by Barnett (1983).

The first EOF explains 36% of the variance in the band-pass winds and is displayed in Fig. 9. It depicts large-scale coherent behavior throughout the upper and mid-troposphere from about 20°S to 60°N, with the variations in the equatorial region leading those elsewhere. Fig. 10 presents the amplitude of the correlation between the time series of the EOF and the time series of the band-pass winds at each grid point. As such, the field represents a map of the square root of the fractional variance that the EOF explains in each region. The similarity in the patterns of Figs. 10 and 8a (the correlation between the band-pass winds and M) is striking, with no major qualitative differences except perhaps for the inclusion of a larger, marginally significant Southern Hemisphere component in the EOF correlation map. This close resemblance suggests that the 40–50 day variations in M are the result of a single coherent motion whose spatial structure is as shown by the EOF. As one might expect from the similarity between Figs. 10 and 8a, the time series for the EOF is significantly correlated with the band-pass M series (Fig. 6). A more detailed analysis of the temporal behavior of the phenomenon, particularly with regard to its "seasonality," will be performed as part of a future study.

The second EOF (not shown here) explains 22% of the variance in the band-pass winds and consists primarily of a strong, high-latitude Southern Hemisphere component. It is, therefore, probably better studied with data sources other than that used here.

Finally, we support our results concerning the significance of the Northern Hemisphere "teleconnec-

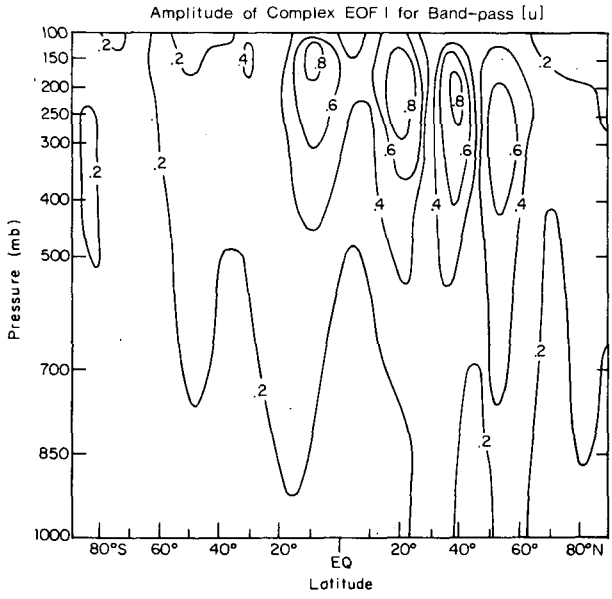

FIG. 9a. Cross section of the amplitude of complex EOF 1 for the Hilbert transform augmented band-pass [u] anomaly field. Values are plotted every 0.2 in arbitrary units.

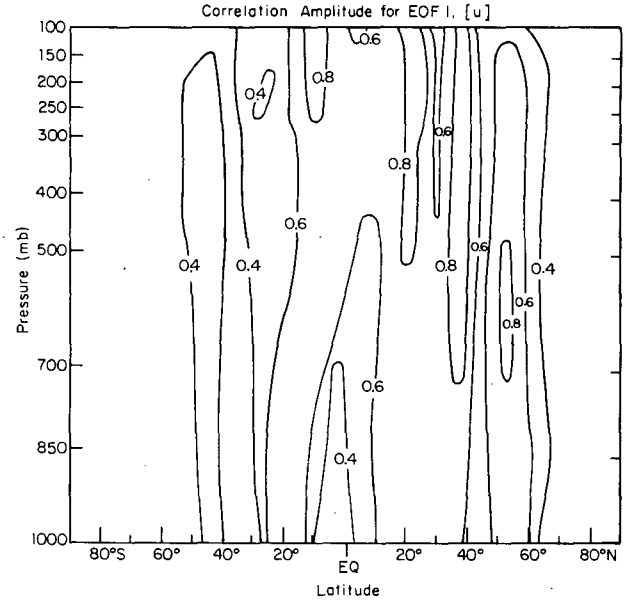

FIG. 10. Cross section of the amplitude of the complex correlation coefficient between the time series of EOF 1 and the band-pass filtered [u] anomalies at each grid point. Only amplitudes judged to be statistically significant, *i.e.*, greater than 0.4, are plotted. The correlation phase is the same as in Fig. 9b.

tion" by computing directly several point-to-point cross spectra with the original broad-band [u] anomaly data. Cross spectra for two pairs of points located in the major centers displayed in Fig. 10 are reproduced in Table 1. These results indicate that the connection between the tropics and the Northern Hemisphere midlatitudes for the 40–50 day fluctuation is indeed a significant one and that most of the variance explained by EOF 1 does result from a single coherent motion.

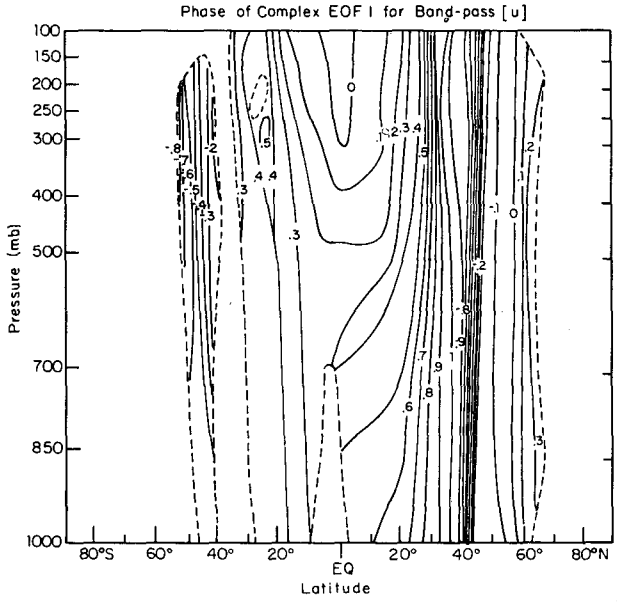

FIG. 9b. Cross section of the phase ($\div\pi$) associated with Fig. 9a. Values are plotted only within the dashed lines where the complex correlation amplitude in Fig. 10 exceeds 0.4.

3. Discussion and conclusions

The character of the 40–50 day variation in the tropics delineated here, including its poleward phase propagation and zonal mean vertical structure, is in good agreement with the description provided by Madden and Julian (1972). The presence of this variation in the zonal mean field is consistent with their suggestion that convection in the western Pacific is being modulated by the eastward phase propagation

TABLE 1. Cross spectra of [u] anomalies for selected pairs of points at periods from 20–80 days. Results are significant at the 95% level of confidence for (coherence)$^2 \approx 0.29$.

Period (days)	20°N, 250 mb vs 37.5°N, 250 mb		37.5°N, 250 mb vs 50°N, 700 mb	
	Coh^2	Phase ($\div\pi$)	Coh^2	Phase ($\div\pi$)
80	0.43	0.93	0.40	−0.95
53	0.52	0.93	0.42	0.95
40	0.69	0.91	0.53	0.80
32	0.47	0.96	0.26	0.92
26	0.12	−0.91	0.25	−0.92
22	0.05	−0.91	0.25	−0.99
20	0.03	0.96	0.22	0.86

of the disturbance. The zonally averaged component can then be viewed as the response of the Hadley circulation to this change in convective forcing. In this light it is interesting to note that although the phase pattern of the tropical component revealed by our EOF analysis (Fig. 9) is symmetric with respect to the equator, the amplitude field is displaced northward, possibly due to the influence of convection in the Pacific Intertropical Convergence Zone. The centering of the phase pattern about the equator may result from the symmetric instability process described by Dunkerton (1981) and Stevens (1983), who demonstrate that flows not symmetric about the equator are inertially unstable. Synoptic evidence of a 30–50 day tropical disturbance that propagates poleward has been offered in a case study by Krishnamurti and Subrahmanyam (1982).

Perhaps the most profound question concerning the tropical component is the cause of the 40–50 day time scale. One possibility, offered by Madden and Julian, is that of a preferred time scale in the forcing, perhaps resulting from a feedback process involving air–sea interactions or latent heat release. Some support for this idea is provided by studies of tropical cloud fields by Yasunari (1980) and Julian and Madden (1981), which indicate that cloudiness and presumably precipitation are modulated on this time scale. Another possibility is that the 40–50 day time scale results from a purely dynamical resonance in the tropical atmosphere's response to random forcing. In this vein a Kelvin wave model has been proposed by Chang (1977) in which the appropriate phase velocity is achieved through the inclusion of cumulus friction parameters and Newtonian cooling. Chang had some success in describing the observed phenomenon as a zonal wavenumber 1 equatorial Kelvin wave, although Stevens and White (1979) have pointed out that the results are very dependent on the specific values chosen for the dissipation parameters. It is hoped that the more detailed description provided here will be useful in evaluating future dynamical models or in determining the vertical structure of the forcing.

Madden and Julian (1972) also observed zonally averaged pressure changes associated with the oscillation and concluded from this that there should be an extratropical component to the motion, although they were unable to find such a signal in surface pressure observations taken in Pacific midlatitudes. Our work, however, does show the existence of a Northern Hemisphere midlatitude component with an equivalent barotropic vertical structure. It is tempting to interpret this feature as a response of the general circulation in midlatitudes to changes associated with the tropical fluctuation. The lack of information in our data set about meridional structure, however, precludes examination of the dynamics of this connection. In particular, it would be interesting to observe the changes in the eddy fluxes of heat and momentum on these time scales.

In conclusion, we have shown that the 40–50 day variation in atmospheric angular momentum is related to the tropical fluctuation described by Madden and Julian. The discovery of a midlatitude Northern Hemisphere component to the variation adds another aspect to this phenomenon, which is still basically rather poorly understood. We hope that our work will encourage future observational and theoretical studies of these motions with the eventual aim of understanding this and other tropical connections with midlatitudes.

Acknowledgments. We are grateful to A. J. Miller of NMC for providing us with most of our atmospheric data and to R. B. Langley for providing us with the lunar laser ranging information. Prof. R. E. Newell and D. A. Salstein offered much useful advice and assistance. J.A. received financial support from M.I.T. Lincoln Laboratory under its staff associate program. Additional support for this study was made available by the Lageos and Crustal Dynamics Projects of the National Aeronautics and Space Administration under Contracts NAS5-25870 and NAS5-27231.

REFERENCES

Anderson, J. R., 1982: Space-time structure of changes in atmospheric angular momentum. S.M. thesis, Dept. Meteor. Phys. Oceanogr., M.I.T., 77 pp.

Barnett, T. P., 1983: Interaction of the monsoon and Pacific trade wind systems at interannual time scales. Part I: The equatorial zone. *Mon. Wea. Rev.*, **111**, 756–773.

Blackman, R. B., and J. W. Tukey, 1959: *The Measurement of Power Spectra.* Dover, 190 pp.

Burg, J. P., 1975: Maximum entropy spectral analysis. Ph.D. thesis, Stanford University, 136 pp.

Chang, C. P., 1977: Viscous internal gravity waves and low-frequency oscillations in the tropics. *J. Atmos. Sci.*, **34**, 901–910.

Chatfield, C., 1980: *The Analysis of Time Series: An Introduction.* Chapman and Hall, 268 pp.

Dunkerton, T. J., 1981: On the inertial stability of the equatorial middle atmosphere. *J. Atmos. Sci.*, **38**, 2354–2364.

Goodman, N. R., S. Katz, B. H. Kramer and M. T. Kuo, 1961: Frequency response from stationary noise. *Technometrics*, **3**, 245–268.

Julian, P. R., and R. A. Madden, 1981: Comments on a paper by T. Yasunari. *J. Meteor. Soc. Japan*, **59**, 435–437.

Krishnamurti, T. N., and D. Subrahmanyam, 1982: The 30–50 day mode at 850 mb during MONEX. *J. Atmos. Sci.*, **39**, 2088–2095.

Langley, R. B., R. W. King, I. I. Shapiro, R. D. Rosen and D. A. Salstein, 1981: Atmospheric angular momentum and the length of day: a common fluctuation with a period near 50 days. *Nature*, **294**, 730–732.

Madden, R. A., and P. R. Julian, 1971: Detection of a 40–50 day oscillation in the zonal wind in the tropical Pacific. *J. Atmos. Sci.*, **28**, 702–708.

——, and ——, 1972: Description of global-scale circulation cells in the tropics with a 40–50 day period. *J. Atmos. Sci.*, **29,** 1109–1123.

Marple, L., 1980: A new autoregressive spectrum analysis algorithm. *IEEE Trans. Acoust., Speech, Signal Process.*, **ASSP-28,** 441–454.

Oppenheim, A. V., and R. W. Schafer, 1975: *Digital Signal Processing.* Prentice-Hall, 585 pp.

Papoulis, A., 1973: Minimum-bias windows for high-resolution spectral estimates. *IEEE Trans. Inform. Theory,* **IT-19,** 9–12.

Rasmusson, E. M., P. A. Arkin, W. Y. Chen and J. B. Jalickee, 1981: Biennial variations in surface temperature over the United States as revealed by singular decomposition. *Mon. Wea. Rev.*, **109,** 587–598.

Rosen, R. D., and D. A. Salstein, 1983: Variations in atmospheric angular momentum on global and regional scales and the length of day. *J. Geophys. Res.*, **88,** 5451–5470.

Stevens, D. E., 1983: On symmetric stability and instability of zonal mean flows near the equator. *J. Atmos. Sci.*, **40,** 882–893.

——, and G. H. White, 1979: Comments on "Viscous internal gravity waves and low-frequency oscillations in the tropics." *J. Atmos. Sci.*, **36,** 545–546.

Weickmann, K. M., 1982: Intra-seasonal fluctuations in near-global-scale modes of circulation and outgoing longwave radiation during Northern Hemisphere winter. Ph.D. thesis, University of Wisconsin, Madison, 107 pp.

Yasunari, T., 1980: A quasi-stationary appearance of 30 to 40 day period in the cloudiness fluctuations during the summer monsoon over India. *J. Meteor. Soc. Japan,* **58,** 225–229.